

THE AUSTRIAN ACADEMY OF SCIENCES' JOINT EXCELLENCE IN SCIENCE AND HUMANITIES (JESH) PROGRAMME

# FIRST PRINCIPLE STUDY OF 2D AND LAYERED MATERIALS

---

DR JELENA PEŠIĆ, RESEARCH ASSISTANT PROFESSOR

INSTITUTE OF PHYSICS BELGRADE, UNIVERSITY OF BELGRADE, SERBIA

# Introduction

---





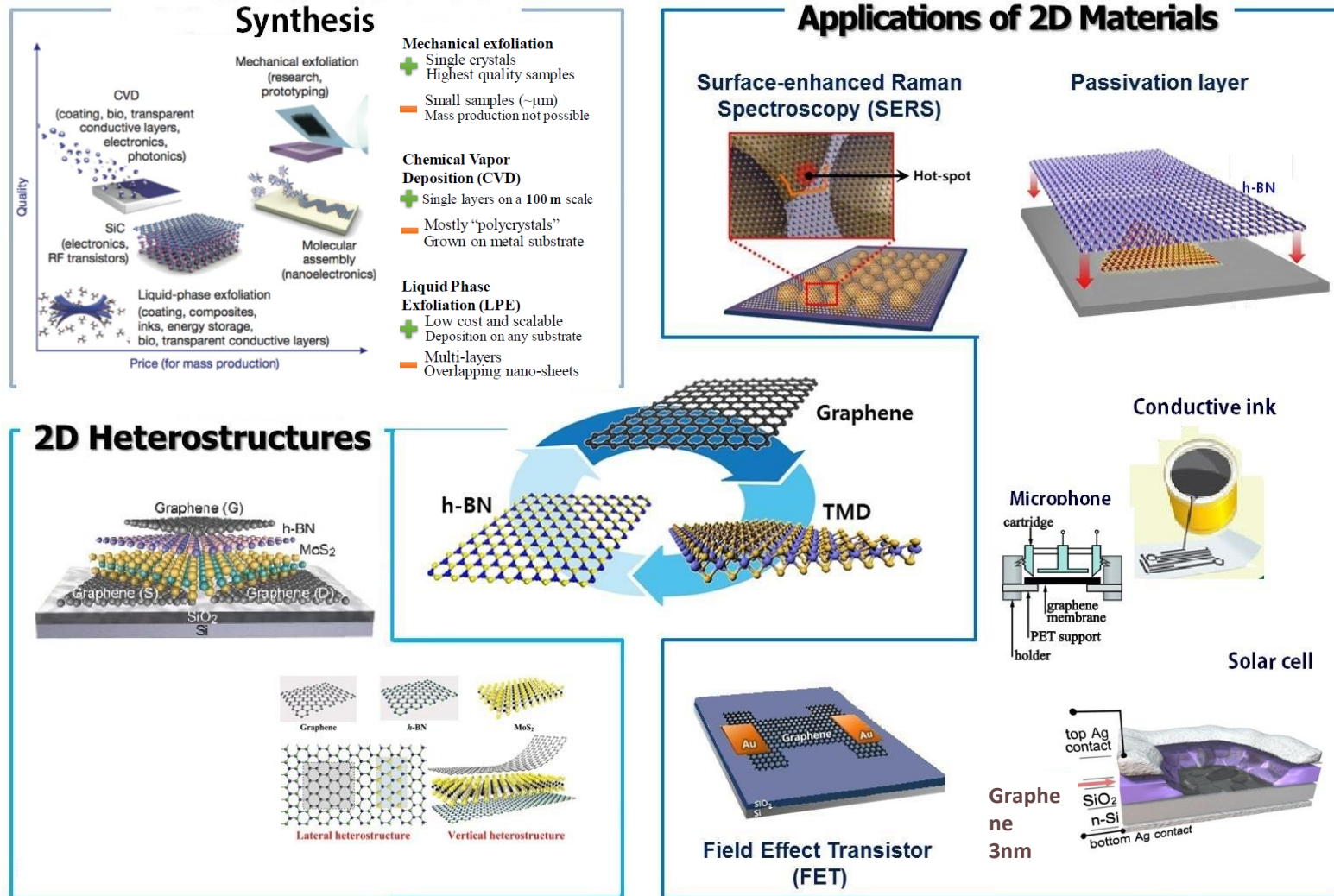
# Introduction

## Institute of Physics Belgrade, University of Belgrade IPB





# Part 1 - Research and applications @Laboratory for 2D materials

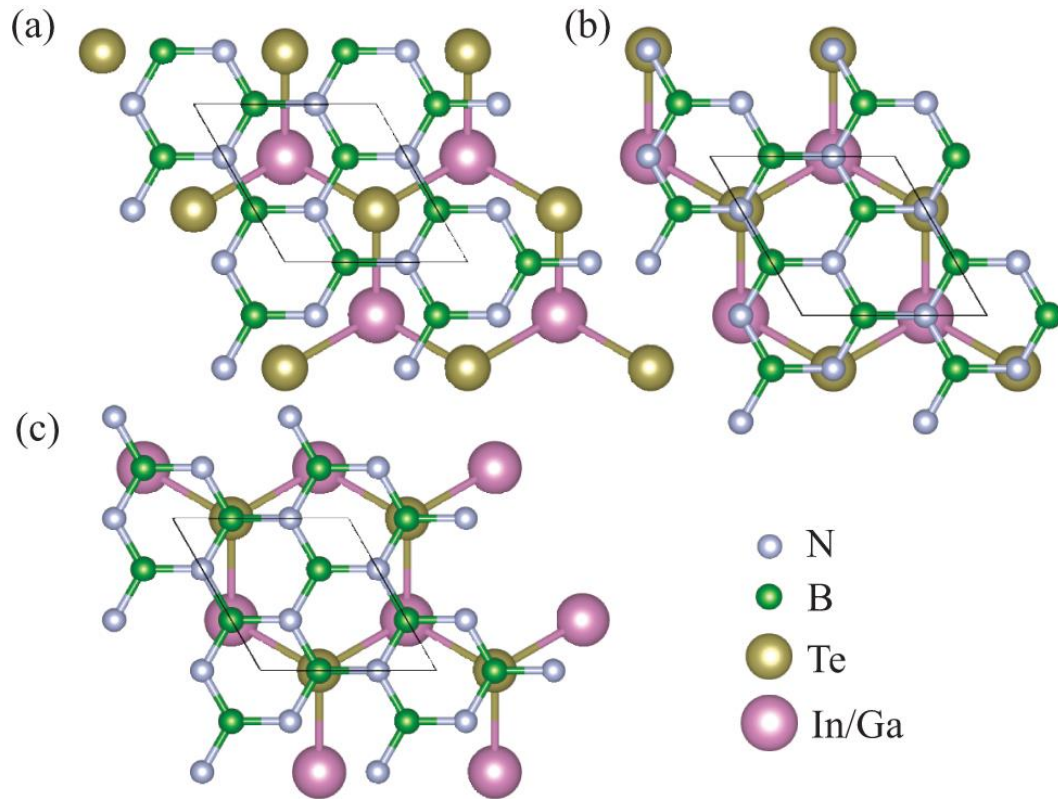


# Layered and 2D materials

---

- tellurides
- iodides
- sulfides and selenides
- other

# NOVEL hBN/In(Ga)Te HETEROSTRUCTURES



hBN/In(Ga)Te heterostructures. Top view of three possible stacking types, (a) H-top, (b) N-top and (c) B-top

Here we present two newly designed vdW heterostructures based on hBN (hexagonal boron nitride) and GaTe or InTe monolayer, in order to make them more robust and resistant to mechanical influences while enhancing their optoelectronic properties. Using density functional theory we investigate electronic and optical properties of those heterostructures.

Our study reveals them as an excellent candidates for various optoelectronic devices with great capabilities of absorption from visible light to far UV part of spectrum, being exceptionally good for absorbing the UV light. The hBN layer is beneficial for mechanical protection of sensitive and vulnerable single layers of monochalcogenides like InTe and GaTe, while as we showed, in our heterostructures, electronic and optical properties are not only preserved but even enhanced.

# Part 2 -Experimental research of 2D and Quasi-2D materials



## Raman spectroscopy system

- Tri Vista 557 spectrometer
- 532 nm line Coherent Verdi G solid state laser
- KONTI CryoVac - 0.5-mm-thick window

### Cryovac Konti Liquid Helium Microscope Cryostat

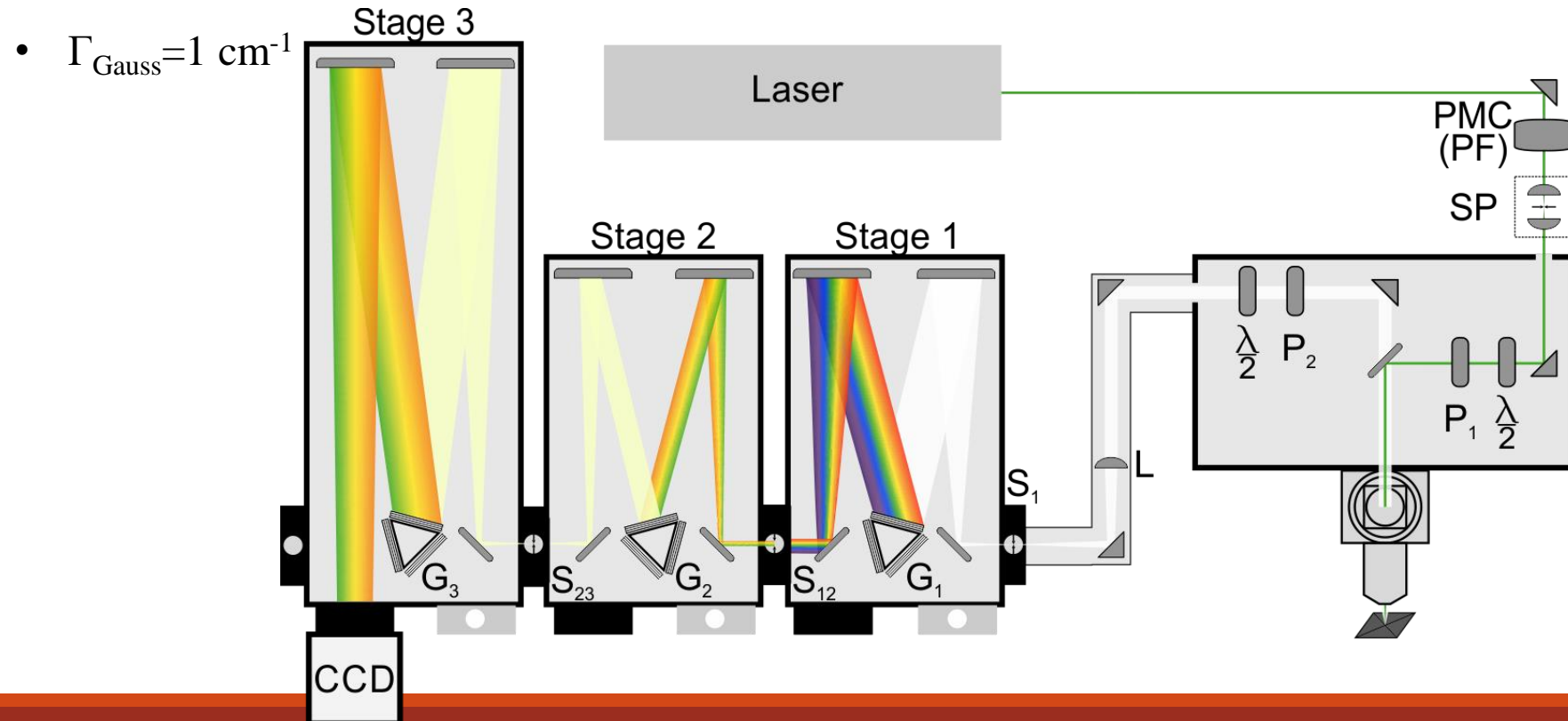
- sample stage with very high stability
- temperature range 3.5-325 K
- temperature stability  $< 0,1$  K
- small footprint and low weight of only  $\sim 2,5$ kg
- small dimensions, height only 45 mm
- sample in vacuum
- adjustable sample holder
- min. distance window-sample 1 mm
- quick and easy sample changes
- windows optical quartz



# Raman spectroscopy system

## Tri Vista 557 spectrometer

- backscattering micro-Raman configuration
- 1800/1800/2400 grooves/mm diffraction grating combination
- measurements under high vacuum ( $10^{-6}$  mbar)



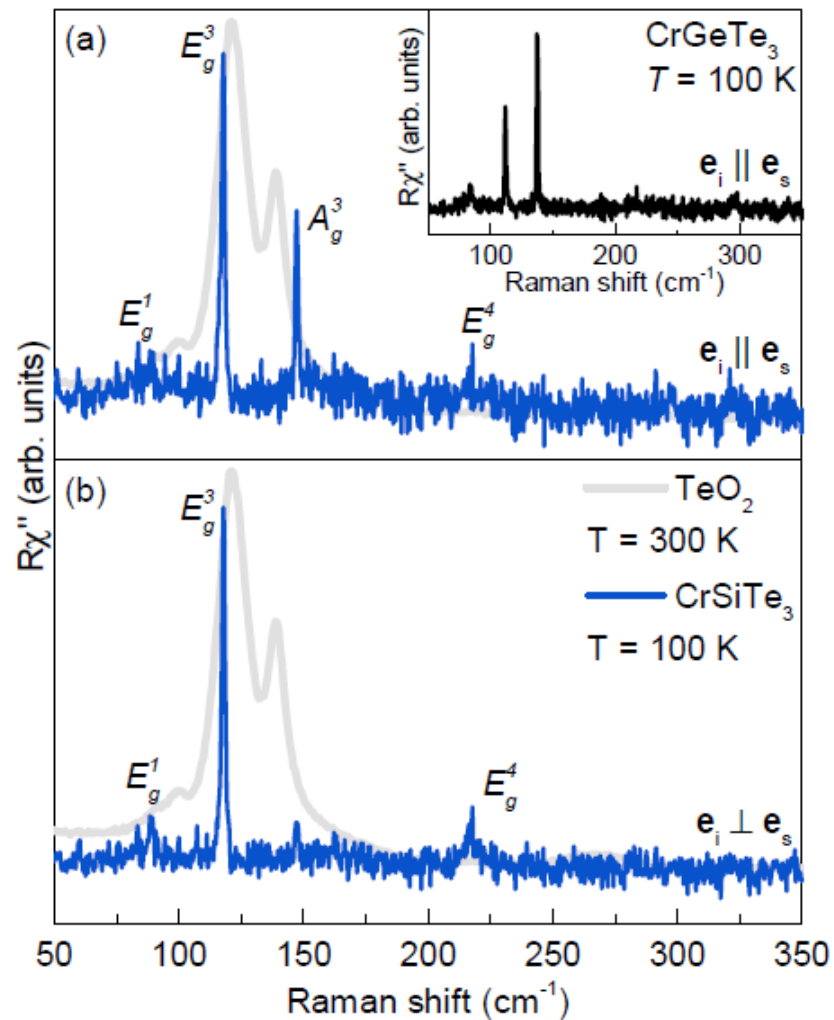


# CrSi/GeTe<sub>3</sub>

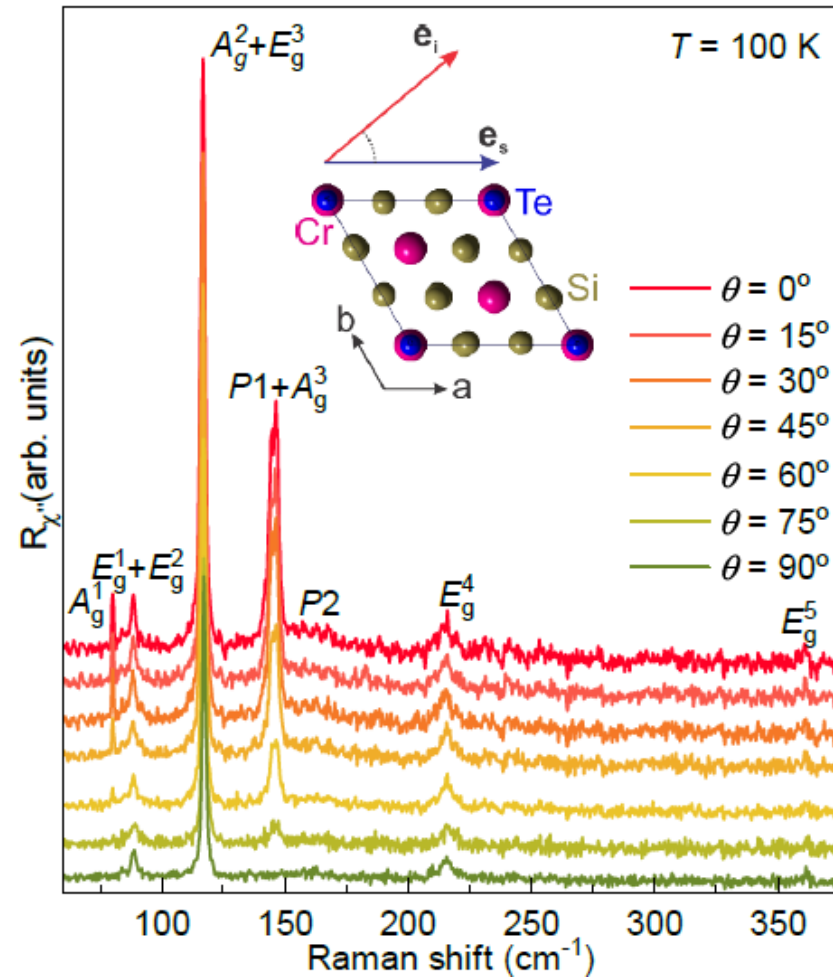
---

EVIDENCE OF SPIN-PHONON COUPLING

Evidence of spin-phonon coupling in CrSiTe3  
 A. Milosavljević, A. Šolajić, J. Pešić, Yu Liu (刘育), C. Petrovic, N. Lazarević, and Z. V. Popović Phys. Rev. B 98, 104306 2018

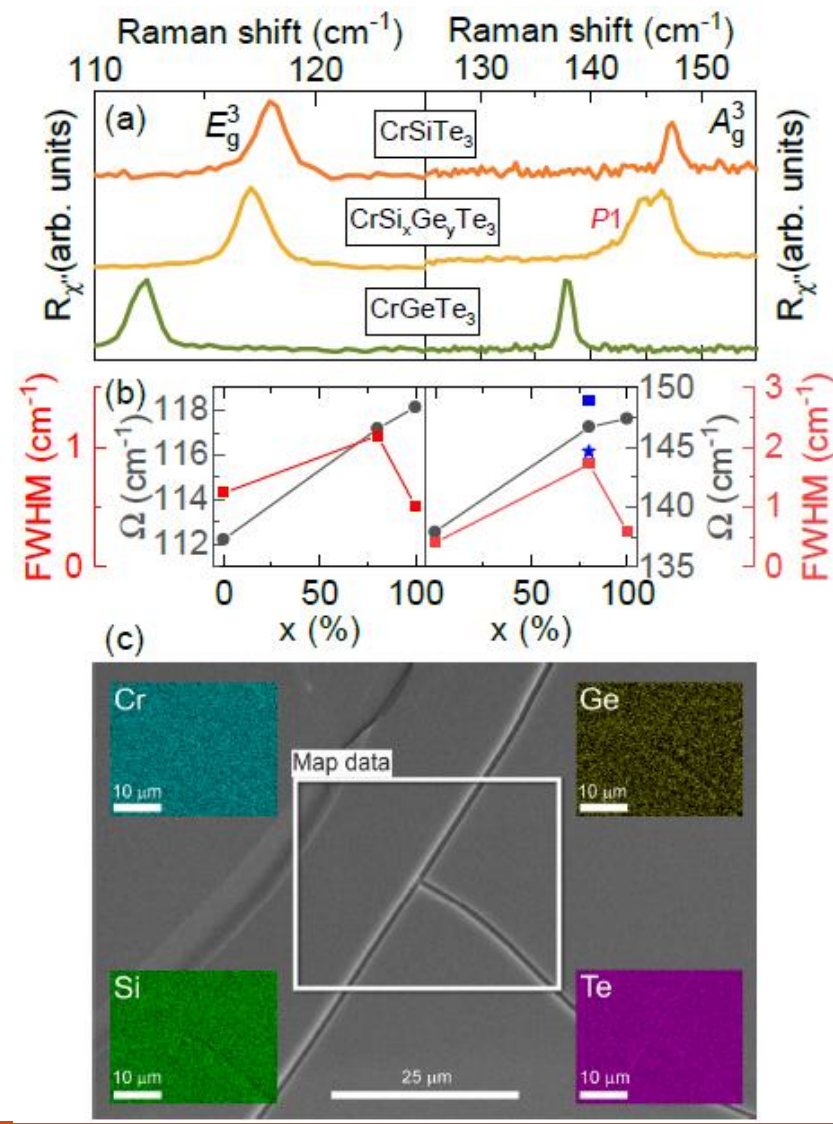


Vacancies and spin–phonon coupling in CrSi0.8Ge0.1Te3  
 A. Milosavljević, A. Šolajić, B. Višić, M. Opačić, J. Pešić, Y. Liu, C. Petrovic, Z. V. Popović, N. Lazarevic - J Raman Spectrosc. 51:2153–2160 2020



Results – Mode assignation in CrSiTe3 and CrSi0.8Ge0.1Te3

Evidence of spin-phonon coupling in CrSiTe3  
A. Milosavljević, A. Šolajić, J. Pešić, Yu Liu (刘育), C. Petrovic, N. Lazarević, and Z. V. Popović Phys. Rev. B 98, 104306 2018



Vacancies and spin–phonon coupling in CrSi0.8Ge0.1Te3  
A. Milosavljević, A. Šolajić, B. Višić, M. Opačić, J. Pešić, Y. Liu, C. Petrovic, Z. V Popović, N. Lazarevic - J Raman Spectrosc. 51:2153–2160 2020

DFT Calculations

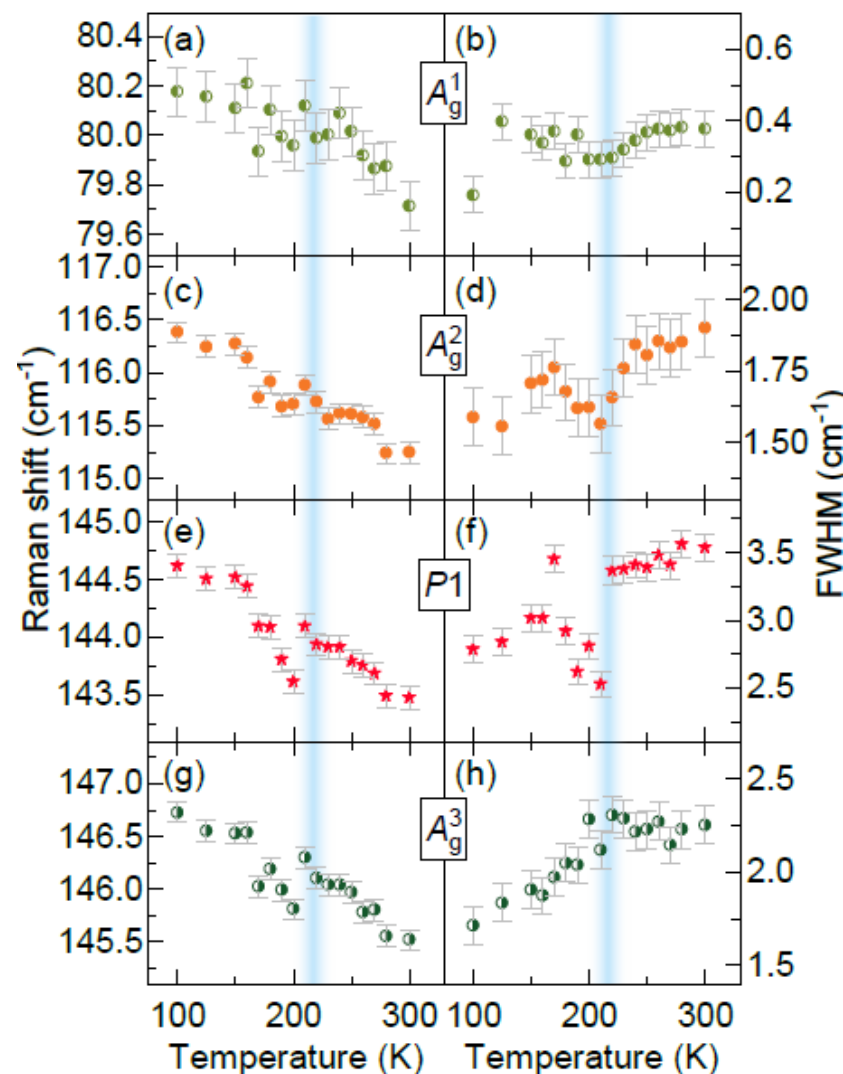
Raman active modes			
Sym.	Calculations		Experiment
	CrSiTe <sub>3</sub>	CrGeTe <sub>3</sub>	CrSi <sub>x</sub> Ge <sub>y</sub> Te <sub>3</sub>
A <sub>g</sub> <sup>1</sup>	88.2	84.2	80.2
E <sub>g</sub> <sup>1</sup>	93.5	82.0	84.5
E <sub>g</sub> <sup>2</sup>	96.9	90.8	88.3
E <sub>g</sub> <sup>3</sup>	118.3	114.2	117.2
A <sub>g</sub> <sup>2</sup>	122.0	105.9	116.4
A <sub>g</sub> <sup>3</sup>	148.0	134.8	146.7
A <sub>g</sub> <sup>4</sup>	208.7	200.3	-
E <sub>g</sub> <sup>4</sup>	219.5	209.6	215.0
E <sub>g</sub> <sup>5</sup>	357.4	229.8	361.1
A <sub>g</sub> <sup>5</sup>	508.9	290.7	-

SEM Measurements

Cr:Si:Ge:Te = 1:0.8:0.1:3



## Temperature dependence in $\text{CrSi}_{0.8}\text{Ge}_{0.1}\text{Te}_3$



- By heating the sample from 100 K to approximately 210 K, monotonous decrease in energy of all the  $A_g$  symmetry modes is present, dominantly driven by thermal expansion.
- Around 210K these modes exhibit sudden increase in energy, followed by a continuous decrease up to room temperature. At the same temperature (210 K), deviation from expected anharmonic type of behaviour is observed for all the  $A_g$  symmetry modes linewidth, with the effect being more pronounced for higher energy modes where the anharmonicity is expected to be higher.
- Having in mind previously reported strong spin-phonon coupling in  $\text{CrSiTe}_3$  believe that this unconventional behaviour of energies and linewidths can be attributed to the coupling of the phonon modes to the spin system

## CrSi<sub>0.8</sub>Ge<sub>0.1</sub>Te<sub>3</sub>

---

- ✓ We performed Raman scattering measurements on pure and doped van der Waals ferromagnets CrSiTe<sub>3</sub> and CrSi<sub>0.8</sub>Ge<sub>0.1</sub>Te<sub>3</sub>
- ✓ CrSiTe<sub>3</sub>
  - ✓ One of E<sub>g</sub> modes shows a clear Fano resonance at lower temperatures
  - ✓ In addition, temperature dependence of all analysed modes deviates from standard anharmonic indicating persistence of magnetic correlations up to 180 K
- ✓ CrSi<sub>0.8</sub>Ge<sub>0.1</sub>Te<sub>3</sub>
  - ✓ Additional peaks *P1*, *P2* and *P3* with pure A<sub>g</sub> symmetry are revealed.
    - ✓ *P1* as a consequence of Ge atoms deficiency
    - ✓ *P2* and *P3* as overtones
  - ✓ Temperature dependence of all analysed modes deviates from standard anharmonic indicating persistence of magnetic correlations up to 210 K

# $\text{VI}_3$ and $\text{CrI}_3$

---

VIBRATIONAL PROPERTIES

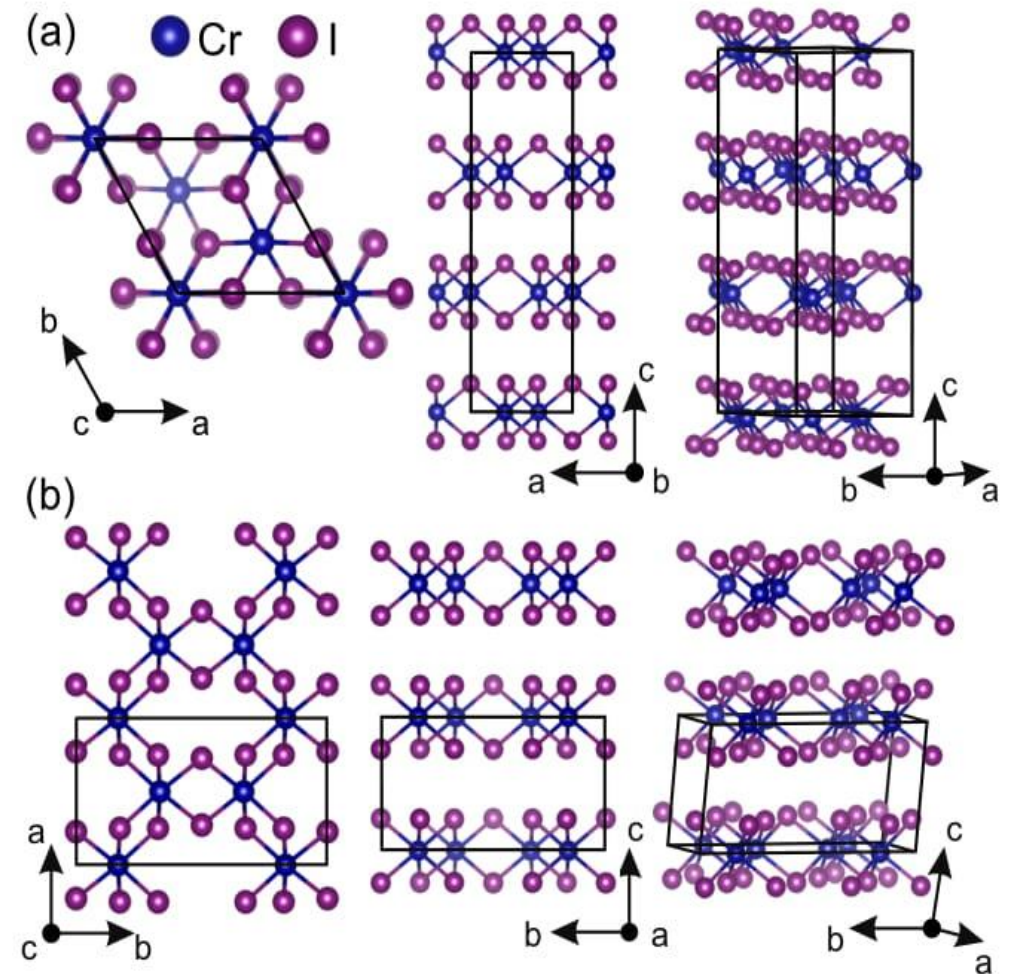


# CrI3

## Lattice dynamics and phase transition in CrI3 single crystals

S. Djurdjić-Mijin, A. Šolajić, J. Pešić, M. Šćepanović, Y. Liu (刘育), A. Baum, C. Petrovic, N. Lazarević, and Z. V. Popović Phys. Rev. B 98, 104307, 2018

- Ferromagnetic semiconductor with Curie temperature of 61 K, bandgap of 1.2 eV, and phase transition occurring at 220 K
- Low temperature phase – rhombohedral ( $R\bar{3}$ ) structure
- high temperature phase-monoclinic ( $C2/Cm$ ) structure(b)
- single layer structure  $p\bar{3}1/m$  ( $D_{3d}^1$ )

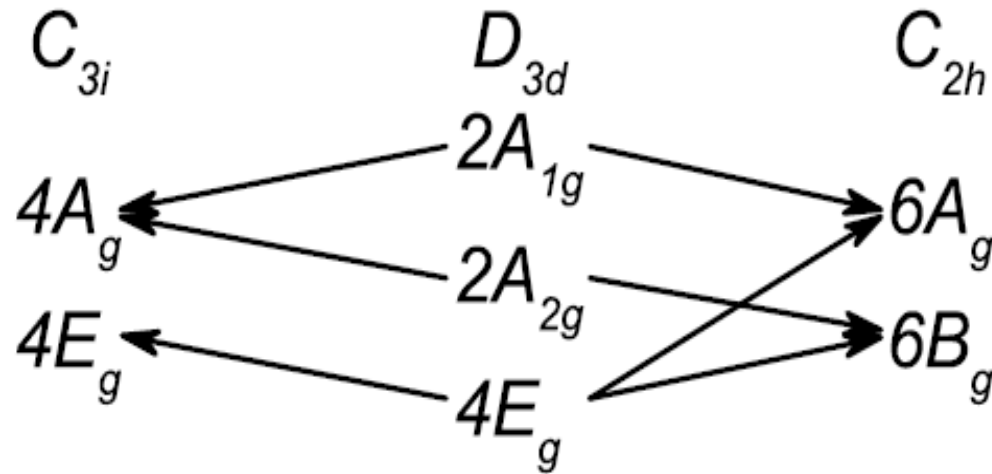


	Space group $R\bar{3}$		Space group $C2/Cm$	
	Calc.	Expt.	Calc.	Expt.
$a$ (Å)	6.87	6.85	6.866	6.6866
$b$ (Å)	6.87	6.85	11.886	11.856
$c$ (Å)	19.81	19.85	6.984	6.966
$\alpha$ (deg)	90	90	90	90
$\beta$ (deg)	90	90	108.51	108.68
$\gamma$ (deg)	120	120	90	90

# CrI<sub>3</sub>

## Lattice dynamics and phase transition in CrI<sub>3</sub> single crystals

S. Djurdjić-Mijin, A. Šolajić, J. Pešić, M. Šćepanović, Y. Liu (刘育), A. Baum, C. Petrovic, N. Lazarević, and Z. V. Popović Phys. Rev. B 98, 104307, 2018



### Symmetry:

- 8 Raman active modes ( $4A_g + 4E_g$ ) -  $R\bar{3}$
- 12 Raman active modes ( $6A_g + 6B_g$ ) -  $C2/m$

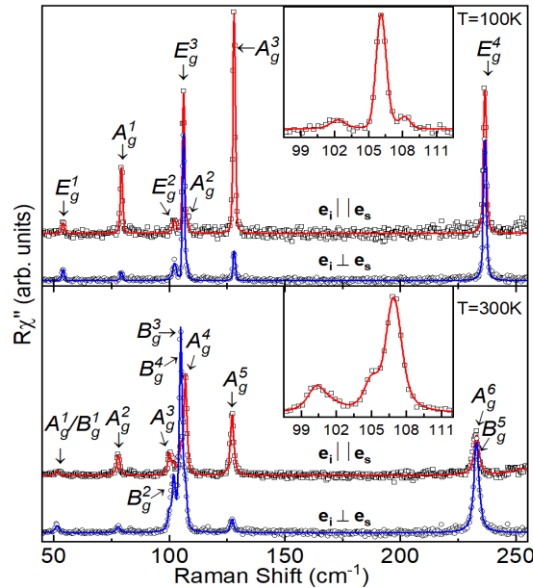
### Experimental results:

- 7 Raman active modes ( $3A_g + 4E_g$ ) -  $R\bar{3}$
- 11 Raman active modes ( $6A_g + 5B_g$ ) -  $C2/m$

Compatibility relations for the CrI<sub>3</sub> layer and the crystal symmetries. In the case of CrI<sub>3</sub>, the symmetry analysis revealed that the single layer structure is fully captured by the  $p\bar{3}1/m$  ( $D_{3d}^1$ ) diperiodic space group DG71, rather than by  $R\bar{3}2m$  as proposed

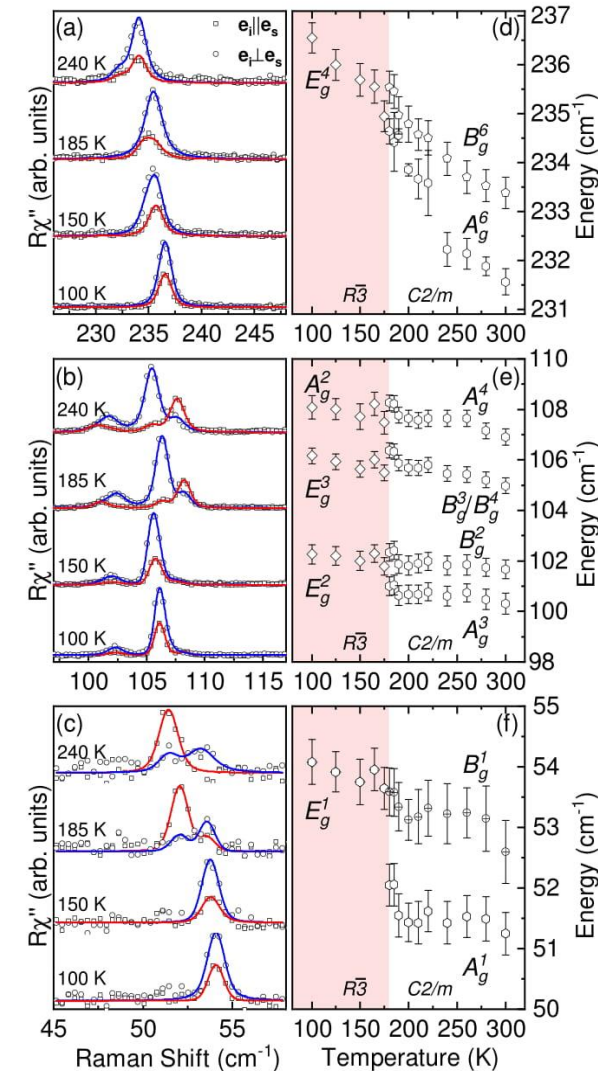
# CrI3

Lattice dynamics and phase transition in CrI3 single crystals  
S. Djurdjić-Mijin, A. Šolajić, J. Pešić, M. Šćepanović, Y. Liu (刘育), A. Baum, C. Petrovic, N. Lazarević, and Z. V. Popović Phys. Rev. B 98, 104307, 2018



Phonon symmetries and phonon energies for the low-temperature  $R\bar{3}$  and high-temperature  $C2/m$  phase of CrI<sub>3</sub>. The experimental values were determined at 100 K and 300 K, respectively. Arrows indicate the correspondence of the phonon modes across the phase transition.

Space group $R\bar{3}$				Space group $C2/m$			
Symm.	Expt. (cm <sup>-1</sup> )	Calc. (cm <sup>-1</sup> )	Calc. (cm <sup>-1</sup> )	Symm.	Expt. (cm <sup>-1</sup> )	Calc. (cm <sup>-1</sup> )	Calc. (cm <sup>-1</sup> )
$E_g^1$	54.1	59.7	53	$B_g^1$	52.0	57.0	52
$A_g^1$	73.33	89.6	79	$A_g^1$	53.6	59.8	51
$E_g^2$	102.3	99.8	98	$A_g^2$	78.6	88.4	79
$E_g^3$	106.2	112.2	102	$A_g^3$	101.8	101.9	99
$A_g^2$	108.3	98.8	88	$B_g^2$	102.4	101.8	99
$A_g^3$	128.1	131.1	125	$B_g^3$	106.4 <sup>a</sup>	108.9	101
$A_g^4$	-	195.2	195	$A_g^4$	108.3	109.3	102
$E_g^4$	236.6	234.4	225	$A_g^5$	106.4 <sup>a</sup>	97.8	86
				$A_g^6$	128.2	131.7	125
				$B_g^5$	-	198.8	195
				$A_g^7$	234.6	220.1	224
				$B_g^6$	235.5	221.1	225



- The splitting of the  $E_g$  phonons into  $A_g$  and  $B_g$  modes at the phase transition is sharp.

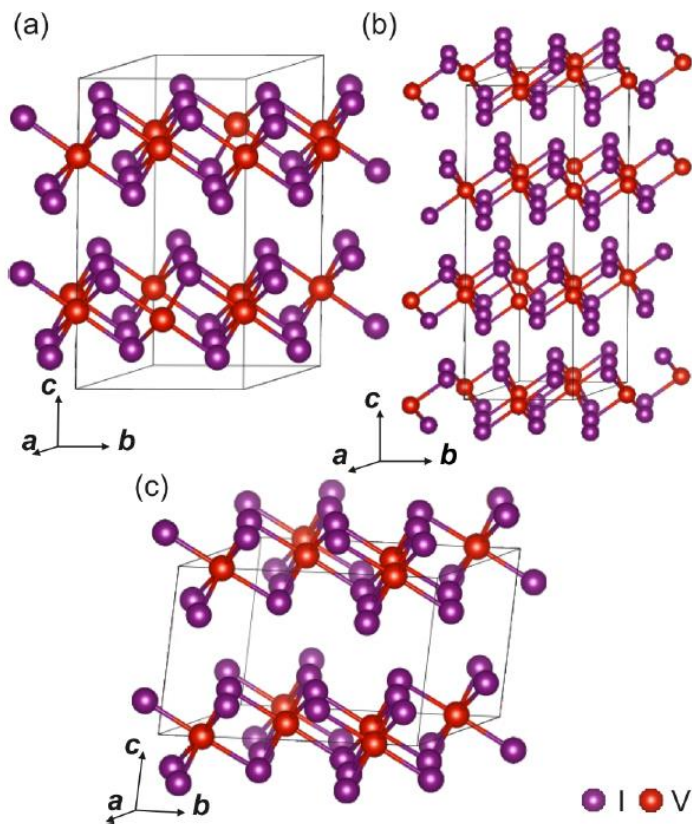
- There are no signs of phase co-existence in the observed temperature range. The maximum temperature interval where the phase coexistence could occur in our samples is approximately 5 K.



# VI<sub>3</sub>

## Short-Range Order in VI<sub>3</sub>

Sanja DjurdjicMijin, A. M. Milinda Abeykoon, Andrijana Šolajić, Ana Milosavljević, Jelena Pešić, Yu Liu, Cedomir Petrovic, Zoran V. Popović, and Nenad Lazarević Inorg. Chem. 2020, 59, 16265–16271



Schematic representation of the high-temperature (a)  $P31c$ , (b)  $R\bar{3}$ , and (c)  $C2/m$  structures of  $VI_3$ . Black solid lines represent unit cells.

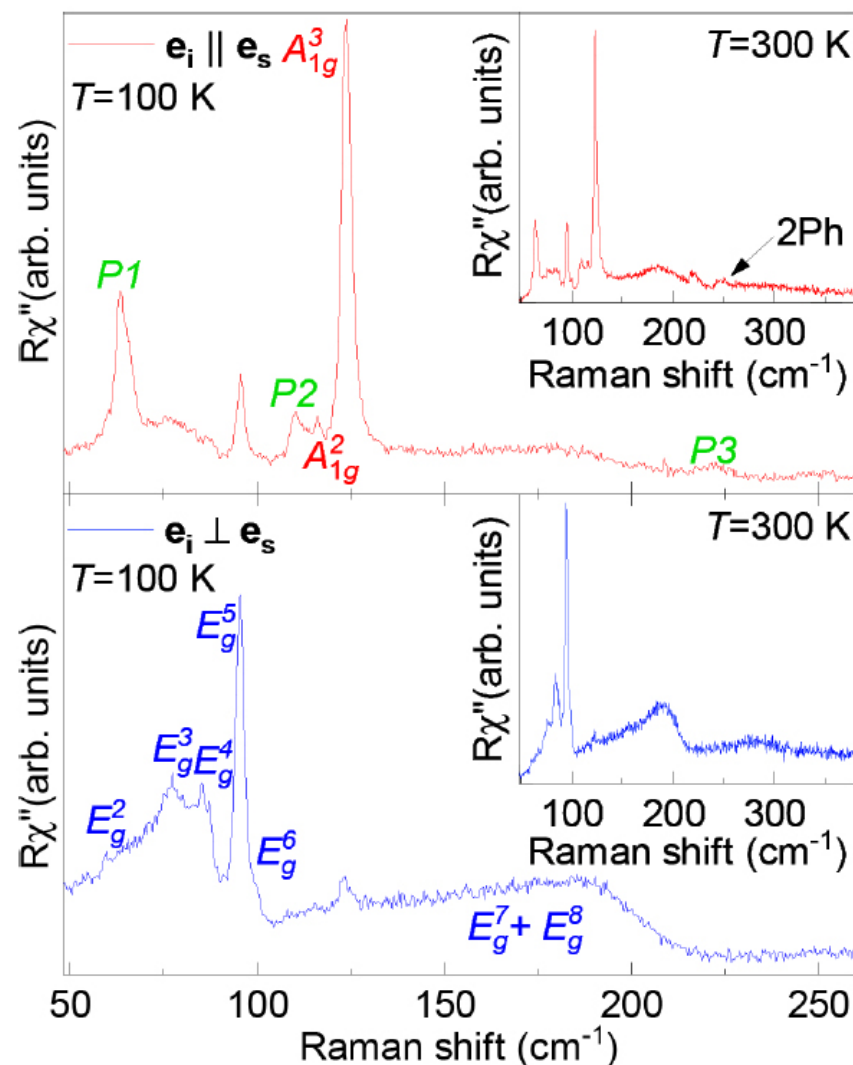
space group $P\bar{3}1c$				space group $R\bar{3}$		space group $C2/m$	
symmetry	calcd (cm <sup>-1</sup> )	calcd (cm <sup>-1</sup> )	exp. (cm <sup>-1</sup> )	symmetry	calcd (cm <sup>-1</sup> )	symmetry	calcd (cm <sup>-1</sup> )
$E_g^1$	17.2	15.2	—	$E_g^1$	45.2	$A_g^1$	58.1
$A_{2g}^1$ (silent)	35.0	56.8		$E_g^2$	69.9	$B_g^1$	60.0
$E_g^2$	62.2	61.6	59.8	$A_g^1$	99.3	$A_g^2$	82.7
$A_{2g}^2$ (silent)	69.4	72.3		$E_g^3$	99.8	$B_g^2$	82.9
$E_g^3$	74.1	75.9	77.2	$A_g^2$	105.1	$A_g^3$	85.7
$A_{1g}^1$	83.3	84.2	—	$A_g^3$	135.5	$B_g^3$	88.9
$E_g^4$	84.9	86.6	86.7	$A_g^4$	167.9	$A_g^4$	99.3
$E_g^5$	91.5	98.4	95.2	$E_g^4$	176.8	$B_g^4$	99.3
$A_{2g}^3$ (silent)	92.2	96.3				$A_g^5$	122.3
$E_g^6$	97.4	108.3	100.4			$B_g^5$	149.9
$A_{1g}^2$	113.2	119.3	116.8			$B_g^6$	161.0
$A_{1g}^3$	117.1	123.9	123.4			$A_g^6$	164.0
$A_{2g}^4$ (silent)	121.3	147.8					
$E_g^7$	132.2	151.9	<i>c</i>				
$E_g^8$	149.4	166.9	<i>c</i>				
$A_{2g}^5$ (silent)	185.9	212.1					

Comparison between Calculated Values of Raman Active Phonon Energies for Insulating and Half-Metallic States of the  $P31c$  Structure and Experimentally Obtained Values (left), and Phonon Symmetries and Calculated Phonon Energies for the  $R\bar{3}$  and  $C2/m$  Structures of  $VI_3$

# VI<sub>3</sub>

## Short-Range Order in VI<sub>3</sub>

Sanja DjurdjicMijin, A. M. Milinda Abeykoon, Andrijana Šolajić, Ana Milosavljević, Jelena Pešić, Yu Liu, Cedimir Petrovic, Zoran V. Popović, and Nenad Lazarević Inorg. Chem. 2020, 59, 16265–16271



Raman spectra of the high-temperature VI<sub>3</sub> single-crystal structure measured in parallel (red solid line) and cross (blue solid line) polarization configurations at 100 K. Peaks observed in both spectra were identified as  $E_g$  modes, whereas peaks observed only in the red spectrum were assigned as  $A_{1g}$  modes. Additional peaks that obey pure  $A_{1g}$  symmetry are marked as  $P1$ – $P3$ .

Room-temperature phonon vibrations of VI<sub>3</sub> stem from the  $P\bar{3}1c$  symmetry of the unit cell. The PDF analysis suggested the coexistence of two phases, short-range ordered  $P\bar{3}1c$  and long-range ordered  $R\bar{3}$ , as two segregated phases and/or as randomly distributed short-range ordered  $P\bar{3}1c$  domains in the long-range ordered  $R\bar{3}$  lattice. Nine of 12 observed peaks in the Raman spectra were assigned in agreement with  $P\bar{3}1c$  symmetry calculations.

Three additional peaks, which obey  $A_{1g}$  symmetry rules, could be explained as either overtones or as activated  $A_{2g}$  silent modes caused by a symmetry breaking. The asymmetry of one of the  $A_{1g}$  phonon modes, together with the anomalous behavior of  $E_{g7}$  and  $E_{g8}$ , indicates strong spin–phonon coupling, which has already been reported in similar 2D materials.



---

PART3-STRAINED FESC- STRAIN EFFECTS IN IRON CHALCOGENIDE  
SUPERCONDUCTORS



# Strained FeSC- Strain Effects in Iron Chalcogenide Superconductors

**Inelastic light scattering study, augmented by scanning probe microscopy (SPM), will be performed on Fe(Se:S) samples in the full doping range at various temperatures and under uniaxial strain**

*Our project is focused on understanding complex interrelations of phases in Fe(Se:S). To this aim, we are working on upgrading and optimizing inelastic light scattering experiment at IPB in the temperature region (6 - 300 K). Furthermore, option of applying uniaxial strain will be implemented*

Discovery of superconductivity in the Fe-based materials (FeBSCs) in 2008 brought new excitement in the field of high-T<sub>c</sub> superconductors. Although much has been learned since, some of the key questions regarding the complex interplay between lattice, magnetism and superconductivity, are still controversial. While posing the challenge, close proximity of the phases in FeBCS can be facilitated through tuning of their properties by applying strain as an additional control parameter [2,3]. Access to the various degrees of freedom can provide the valuable data needed, not only for pinpointing the generic properties and, possibly, understanding of the FeBSCs, but also for material/device engineering.

Inelastic scattering of visible light (Raman effect) has the capability to simultaneously probe lattice, charge and spin excitations as well as their mutual interactions and is well established as an indispensable tool for research into high-T<sub>c</sub> superconductors [4].

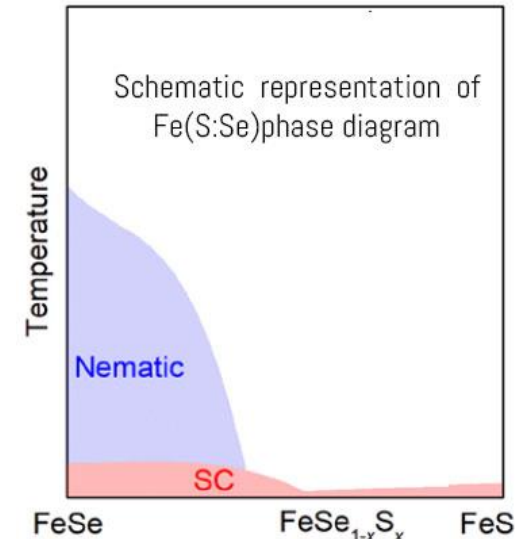
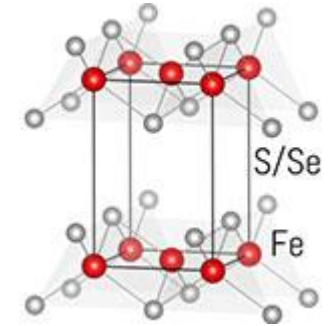
**In FeSe this interplay leads to a symmetry-broken state (often referred to as nematic state) that is characterized by small orthorhombic distortions of the lattice and a large anisotropy of the electronic properties. Nematicity created a lot of excitement since superconductivity may be boosted by the related fluctuations.**

The first objective is to track down possible signatures of the interrelation of the normal, nematic and superconducting states. To this end, lattice, charge and spin excitations in Fe(Se:S) single crystals will be studied spectroscopically as a function of temperature and doping.

The second objective is to scrutinize the influence of a symmetry-breaking strain field on the various phase transitions. It is intended to monitor the effects by Raman studies of Fe(Se:S) single crystals.

Based on obtained results, a possibility for engineering strain devices that exploit properties of iron-chalcogenide superconductors will be explored.

<http://strainedfesc.ipb.ac.rs/>



Project *StrainedFeSC* is financed by the Science Fund of the Republic of Serbia under the grant number 6062656 at Institute of Physics Belgrade Serbia

# ACKNOWLEDGEMENT

---

- Prof Dr Alberta Bonanni, QMAG and Johannes Kepler University,
- The support of the The Austrian Academy Of Sciences' Joint Excellence In Science And Humanities (Jesh) Programme
- Prof Dr Kurt Hingerl and ZONA and Project of bilateral cooperation between Austria and Serbia, by the Ministry of Education, Science and Technological Development of the Republic of Serbia, under number: 451-03-02141/2017-09/31
- The Research “Strain Effects in Iron Chalcogenide Superconductors” was supported by the Science Fund of the Republic of Serbia, PROMIS, No. 6062656, StrainedFeSC
- Funding provided by the Institute of Physics Belgrade through the grant by the Ministry of Education, Science and Technological Development of the Republic of Serbia.
- All calculations were performed using the computational resources at Johannes Kepler University, Linz, Austria.